IJE TRANSACTIONS C: Aspects Vol. 27, No. 6, (June 2014) 829-838

International Journal of Engineering

Journal Homepage: www.ije.ir

Material Flow in Rotary Drums

M. R. Yousefi, M. Shirvani*

Department of Chemical Engineering, Iran University of Science & Technology, ResaltCircle, Tehran, Iran

PAPER INFO

Paper history:
Received 04 September 2013
Received in revised form 10 November 2013
Accepted 12 December 2013

Keywords:
Rotary Drum;
Material Flow
Steady-State Model
Model Error

ABSTRACT

The experimental investigation of material flow in non-flight rotary drums is studied in a pilot scale apparatus. Contrary to the other published references that have used granular materials, the novelty of this work is that fine particles were used in the experiments. The objective of the paper is to declare the errors of steady-state model of material flow in such devices. The operating conditions during experiments were conducted in the range of slumping, rolling and cascading regimes of material flow inside rotary drums. To keep with such conditions the rotation speed, axis inclination and feeding flow rate were considered within the range of 3.33 to 7.00 (rpm), 0.00 to 3.00 (deg.) and 6.80 to 13.60 (g/s), respectively in a drum of 14 cm diameter.The obtained experimental data reveals that the model does not describe well the material flow in feeding zone as well as in the discharge zone. However, it is reasonably well for application in the intermediate sections.

doi: *10.5829/idosi.ije.2014.27.06c.02*

NOMENCLATURE

C_A	Coefficient defined in Equation (2), S	R	Drum radius, m
C_B	Coefficient defined in Equation (2), -	x	Axial direction from feeder, m
D	Inside diameter, m	t	Time, *S*
F_r	Froude number, -	**Greek letters**	
g	Gravitational acceleration, m/s^2	β	Axis inclination of cylindre, deg.
h	Beddepth, m	γ	Statice angle of repose of the bed of material, deg.
j	Filling degree, -	φ	Maximum half angle subtended by the bed at the drum axis, deg.
L	Drum length, *m*	ρ	Bulk density, kg/m^3
N	Rotation speed, rev / s	**Subscripts**	
Q_V	Volumetric flow rate of transmitted solid materials, m^3/s	V	Volumetric
Q_S	Mass flow rate of transmitted solid materials, g / s	S	Mass

1. INTRODUCTION

Flow of solid materials inside rotary drums includes complicated flow patterns. This complexity is due to the axial and radial-angular motions caused by gravity and rotating wall of the drum. These motions are of great importance and impose special effects on the patterns of material flow and operation of the rotary drum. Materials transport in axial direction is important for its contribution to the residence time of the materials inside the drum [1]. For instance, residence time of materials in rotary cement kilns affects the formation and quality of the produced clinker. Axial transport of the bulk of solid materials, depend on parameters like feed flow rate, rotation speed, bed depth (or filling degree) of solid materials, axis inclination and material physical properties including:

*Corresponding Author Email: shirvani.m@iust.ac.ir (M. Shirvani)

particle size, particle density and dynamic angle of repose [1]. Variations in axial velocity directly affect the bed depth in the bulk of materials. A lot of studies have been contributed to the axial and transversal motions of materials in rotary drums. A traditional practice in modeling and simulating rotary drums is that the bed depth of materials is supposed to be constant along the drum [1, 2]. This approximation results in constant retention time and constant axial velocity of materials in the drum. Experimental and computational attempts in modeling and predicting of steady state axial motion and bed depth of materials in rotating drums have been devoted by Kramers and Crookewit [3], Perron and Bui [4], Spurling et al. [5]. In this paper, we are referring frequently to the model of Kramers and Croocewit [3]. Thus, for the sake of simplicity, it is abbreviated as K-C model all through the paper. Specht et al. [6] have tried to introduce corrections to the model of Kramers and Croockewit [3] for the discharge zone of the drums. Due to the trivial effect the model of K-C does not consider the counter flow of gas stream on material flow [7]. However, since this effect is negligible on the hold up of materials, the model of K-C is known as a useable model in simulating the steady-state bed depth profile of materials inside the drums. Lebas et al. [8], published the experimental data of bed depth and residence time for a 0.60 (m) in diameter drum and compared their results with the model of K-C. Their report reveals that a good adaptation existed between the model and data. Experimental investigations performed by Mujumdar [9], concerning to fitness of the model of K-C has revealed that the model is reasonably good in predicting, at steady-state and investigation of the effects of variations in feed flow rate and rotational speed on bed depth. Material motion in transversal direction is important in homogeneity of the product. With increase of rotational speed, six different flow regimes [10], can be recognized in a rotary drum. These are affected by material physical properties, diameter of drum, axial inclination, operating variables including: feeding rate and rotational speed, rate of heat and mass transfer between gas and solid material, and mixing intensity in the bed of materials. Slumping, rolling and cascading flow regimes are used widely in industries. The slumping regime appears at slow rotation speeds (less than 3% of the critical speed of rotation). Rolling and cascading regimes appear at 3 to 30% of critical speed of rotation.

2. THEORY

The model of Kramers and Croockewit [3], for material flow in various cross sections of rotary drums is shown in Equation (1). This equation represents the relation between volumetric flow rate of solid materials, Q_v; and operating variables of rotary drums at steady-state condition. The operating variables include axis inclination of the drum, β; Static angle of repose of thematerial, γ; radius of the drum, R; rotation speed , n; bed depth of materials, h and the distance from discharge end , x.

$$Q_V = \frac{4\pi nR^3}{3}\left(\frac{\tan(\beta)}{\sin(\gamma)} + \frac{dh}{dx}\cot(\gamma)\right)\times\left(2\frac{h}{R} - \left(\frac{h}{R}\right)^2\right)^{\frac{3}{2}} \quad (1)$$

Equation (1) can be written in the form of Equation (2) wherein C_A and C_B are two variables depending on the parameters: β, γ and n .

$$\frac{dh}{dx} = C_A Q_V((2R-h)h)^{\frac{-3}{2}} - C_B \quad (2)$$

$$C_A = \frac{3\tan\gamma}{4\pi n} \quad , \quad C_B = \frac{\tan\beta}{\cos\gamma} \quad (3)$$

As boundary condition for Equation (2), K-C model, assumed that, when no dam is present to the flow of materials the bed depth of materials is equal to the size of a single particle (near to zero) at discharge end of the drum. The conditions of ring build up or material clogging in rotary drums is referred to as “dam”in the literature. Thus, the boundary condition in Equation (2) for the condition of no dam existing in the passage of material flow is:

$$h(x=0) = h_0 \quad (4)$$

where, h_0, is taken as a very small value. It should be noted that $x = 0.0$ is considered for the discharge end of the drum. Specht et al. [6], showed that the bed depth of material at the discharge section is much larger than a single particle size. They introduced the dimensionless, Bed Depth Number, in place of the single particle size. However, they did not develop a model with their own boundary condition. Heinen at al. [9], have defined the critical rotation speed as:

$$n_c = \frac{60}{2\pi}\sqrt{g/R} \quad (5)$$

In rolling regime, the bed depth of material appears at lower rotational speeds compared to cascading regime. In the experiments performed in this work the operating conditions during experiments was conducted in the range of slumping, rolling and cascading regimes. These are particularly used in rotary cement kilns as well as many other rotary drums. In this work, the experiments were conducted in the range of variables corresponding to the slumping, rolling and cascading regimes that are most applicable in the industries.

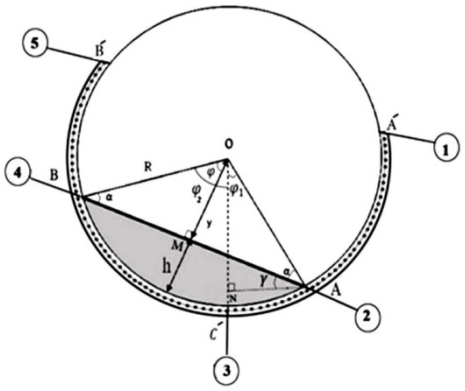

Figure 1. Cross section of the rotary drum including the frame of optical sensors. 1) First sensor around the drum; 2) Initial point of material bed; 3) Reference sensor in the bottom of drum; 4) End point of material bed; 5) End sensor around the drum

The objective of the paper is to investigate the validity of the steady-state model of material flow in rotary drums in different zones of the apparatus used in the experiments. The results are reported in detail in the relevant tables.

Variables including filling angle, of materials and the dynamic angle of repose of material have significant importance when material transport is considered in rotary drums. The relations provided in this section illustrate the way of calculating these parameters at a cross section like the one which is shown in Figure 1. This figure shows a cross section around which the optical sensors are installed in a fixed and stationary ring type frame such that the drum slides and rotates inside it.

According to this figure, filling angle can be calculated by measuring the length of arc

$$BA = BC' + C'A$$
$$\varphi = \frac{1}{2R}(BC' + C'A) \quad (6)$$

Bed depth of materials, filling degree and dynamic angle of repose can be calculated from filling angle as indicated in Equations (7), (8) and (9), respectively.

$$h = R(1 - \cos\varphi) \quad (7)$$

$$j = \frac{1}{\pi}\left(\varphi - \frac{1}{2}\sin 2\varphi\right) \times 100 \quad (8)$$

$$\gamma = \varphi - \varphi_1 \quad (9)$$

The dimensionless Froude number, used for determining flow regime is calculated from rotation speed and drum radius as:

$$Fr = \frac{(2\pi n)^2 R}{g} \quad (10)$$

Variations in accumulation of materials at any cross section of the drum can be determined by continual measurement of points "A" and "B" in Figure 1. These points are measured with reference to the fixed point "C'" by a series of optical sensors under the light of a projector mounted over them. From the measurements of "A" and "B" all the other required parameters can be calculated using the relations in the above. The mathematical details of the above equations are provided in appendix A.

3. APPARATUS

The rotary drum used in the experiments was made from transparent plastic material to provide the possibility of measuring and monitoring the variations in the filling angle (or bed depth) by optical sensors installed around the desired cross section. In the following section, the basic geometric relations required for calculations are presented. Figure 2 shows a scheme of the drum with the optical sensors and projectors. Experimental apparatus includes a transparent rotating drum of 14 cm inside diameter and 195 cm length ($L/D = 13.9$), adjustable in axis inclination, with programmable gear-motors for feeding and rotating the drum, and the lateral equipments including: feed and discharge storage tanks, drum inclination regulating motor and the other facilities for materials transport between discharge and feed storage tanks. Other auxiliary equipments including dust removal cyclone and bag filter, as well as the draft fan were provided for material transportation from discharge tank to storage tank. For creating surface friction and prevention of solid materials from gliding on the inner wall, longitudinal narrow bands in 3 mm width and 1 mm thickness made of transparent plastic material were stick on the inner wall surface of the drum in distances of about 30 mm from each other. Material feed flow rate as well as rotation speed variables are adjustable. In this way, desired inputs such as: step input, as well as pulse and periodical inputs in feed flow rate and rotation speed can be applied in order to study the dynamics of material transport in the drum.

Two different types of powder materials were used in the experiments with the specifications listed in Table 1. The results of experiments for determining the effects of axis inclination and rotational speed and feed flow rate on bed depth of material were the same for both of materials used.

The motors used for feeding and rotating the drum, as well as the motor for adjusting the axis inclination were programmable by PLC to be adjusted and programmed in their rotation speed. Optical sensors were used in different sections of the drum to measure the variations of bed depth of materials that can be used for determination of other required parameters.

All geometric parameters at any specified cross section could be calculated by measuring the two end points of the upper surface of the bed of materials designated by points A and B in Figure 1. For this purpose, a series of photo resistors made from cadmium sulfide connected in series, with 0.10 mm resolution, were used. The obtained data from optical sensors were processed by the PLC. Three sets of 500 watt projectors were employed as light sources that were adjustable axially to be put over the sensor locations in different cross sections along the drum. Moreover, the apparatus was covered by a curtain around it to provide dark room condition for preventing sensors malfunctioning affected from outdoor lights. This also provides, a reference light condition for calibrating the measuring system; that can be done by use of the measurements from straight readings of points A and B from outside of the drum.

4. EXPERIMENTS

Steady-state condition of the drum was established by use of an electronic balance located at the discharge end of the drum to check the equality of the flow rates at inlet and outlet. By measuring the filling angle of materials in various cross sections the data of steady-state condition of the drum were obtained and checked with the model of K-C in Equation (1). The results of some experiments conducted for investigating the effects of operating variables on steady-state material bed depth without dam are presented in the following sections. The operating variables applied in experiments include axis inclination, rotation speed and feeding rate to the drum. In the next sections of the paper, the results of experiments and model simulations are presented.

TABLE 1. Specifications of the material used in the experiments

Powder	Silica Grinded Zeoli	Grinded Zeolite Catalyst
Mean Particle size (mm)	0.244	0.152
Density (kg/m^3)	2580	2390
Angle of repose	$30^\circ \pm 0.5^\circ$	$32^\circ \pm 0.5^\circ$

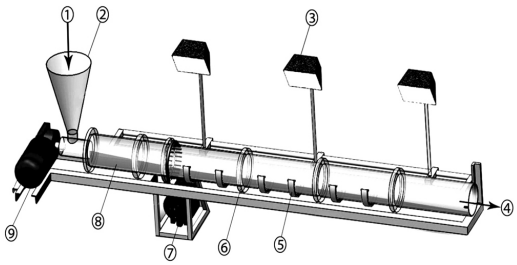

Figure 2. Transparent rotary drum and the adjacent equipment. 1) Materials input; 2) Materials storage hopper; 3) Projector; 4) Materials output; 5) Optical sensor; 6) Gear motor for drum rotation; 7) Bed depth of materials; 8) Feeding motor

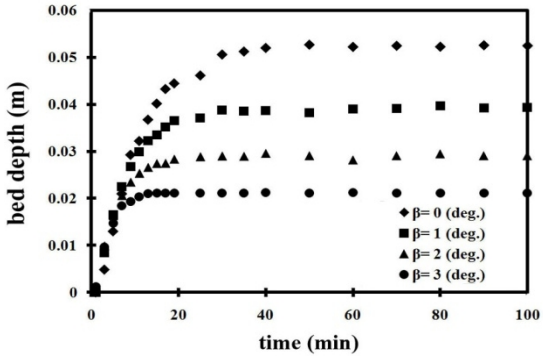

Figure 3. Variation of spent time with axis inclination for the bed depth to reach to steady state, at 60 cm distance from feeding zone.
$Q_s = 10.33\left(g/s\right)$, $\gamma = 30 \pm 0.5(\text{deg.})$, $n = 6.00\left(rpm\right)$,
$\rho = 2580\left(kg/m^3\right)$, $sensor\ \ location = 0.60(m)$

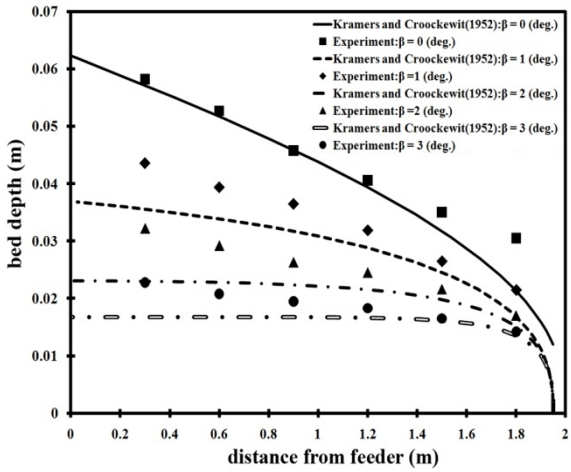

Figure 4. Comparison of predicted values of bed depth profile by the model of K-C with experimental data (variation of axis inclination).
$Q_s = 10.33\left(g/s\right)$, $\gamma = 30 \pm 0.50(\text{deg.})$,
$n = 6.00\left(rpm\right)$, $\rho = 2580\left(kg/m^3\right)$

5. EFFECT OF AXIAL INCLINATION

In the first series of experiments, the effects of each of the operating variables were investigated with the others being constant. This was done in the fixed longitudinal cross section of 60.00 (cm) distance from the feeding section. In these experiments, the sensors were located in the designated section. The variation of bed depth was measured with increase of time until establishment of steady state condition was achieved. Experiments conducted for the effect of axis inclination were carried out at 10.33 (g/s) of feed flow rate and 6.00 (rpm) rotation speed. Figure 3 shows the variation of bed depth of materials with time at 60.00 (cm) distance from feeding section for various angles of axis inclination, starting from empty drum condition up to achievement of steady state condition. This figure shows the trend of decreasing of the spent time for establishment of steady state condition with increase of axis inclination.

Figure 4 compares the results of simulating the material bed depth profile from the model of K-C with the data at 6.00(rpm) rotation speed and 10.33 (g/s) feed flow rate for various axis inclinations. As is shown in the figure, the fitness improves with reduction of axis inclination.

Table 2 is provided for better recognition of the trend of variations of errors between the model of K-C and data in different sections of the drum. It shows that the least error appears at zero axis inclination, while the error increases up to a maximum point at moderate axis inclinations. This is true, also, for near to feeding zone regions. However, the results are reverse for discharge zone, since with increase of axis inclination the model error decreases. Actually, it can be straightly inferred that with decreasing of the bed depth in the discharge zone the error of the K-C model will decrease. This is relating to the fact that the bed depth boundary condition of the K-C model approaches more to reality with decrease of bed depth at discharge section. Therefore, since the increase of axis inclination results in reduced bed depths along the drum, then the discharge zone predictions of the model, also, improves with increase of axis inclination.

6. EFFECT OF ROTATION SPEED

The same results as of varying inclination can be observed for variation of rotation speed. Experiments in this series are performed at fixed values of 1.00(deg.) axis inclination and 10.33(g/s) feeding rate. Rotation of the drum produces two speed components in material flow, one in axial direction and the other in transversal direction. Increasing transversal component of material motion results in variation of flow patterns in transversal direction of the drum, and causes mixing phenomenon in transversal section to be strengthened.

Figure 5 shows the variation of bed depth of materials with time at 60.00 (cm) distance from feeding section for various amounts of rotation speed, starting from empty drum condition up to achievement of steady state condition.

Figure 6 compares the results of simulation of the steady state model of K-C with the obtained data at 1.00 (deg.) axis inclinations and 10.33(g/s) feeding rate. Comparison of data with model predictions show that better fitness is achieved at lower rotation speeds.

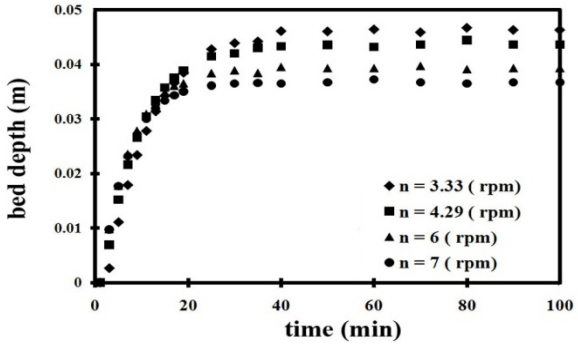

Figure 5. Variation of spent time with rotation speed for material bed depth to reach to steady state, at 60 cm distance from feeding zone.
$Q_s = 10.33(g/s)$, $\gamma = 30 \pm 0.50(\text{deg.})$, $\beta = 1.00(\text{deg.})$,
$\rho = 2580(kg/m^3)$, $sensor\ \ location = 0.60(m)$

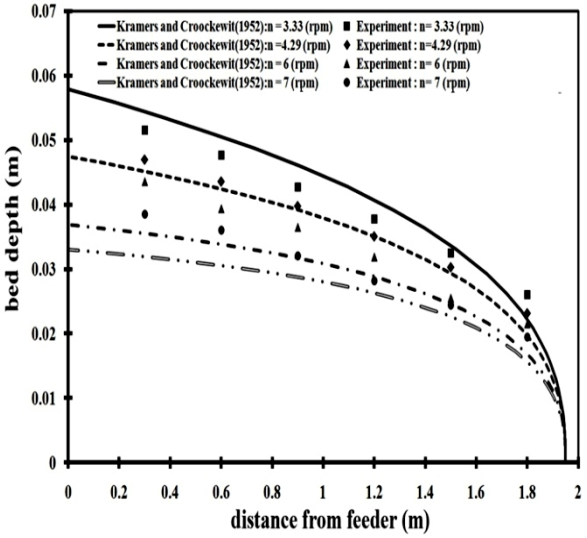

Figure 6. Comparison of predicted values of bed depth profile by the model of K-C with experimental data(variation of rotation speed).
$Q_s = 10.33(g/s)$, $\gamma = 30 \pm 0.50(\text{deg.})$,
$\beta = 1.00(\text{deg.})$, $\rho = 2580(kg/m^3)$

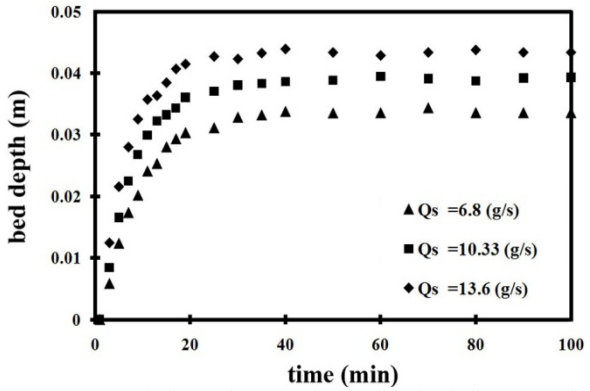

Figure 7. Variation of spent time with feed flow rate for material bed depth to reach to steady state, at 60 cm distance from feeding zone.
$Q_s = 10.33(g/s)$, $\gamma = 30 \pm 0.50(\text{deg.})$, $\beta = 1.00(\text{deg.})$,
$n = 6.00(rpm)$, $\rho = 2580(kg/m^3)$, $sensor\ \ location = 0.60(m)$

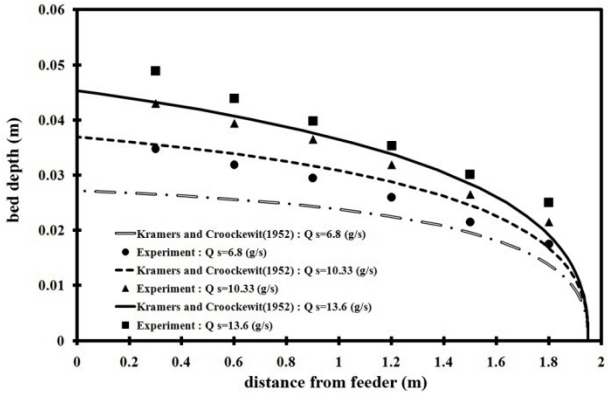

Figure 8. Comparison of predicted values of bed depth profile by the model of K-C with experimental data (variation of feed flow rate).
$Q_s = 10.33(g/s)$, $\gamma = 30 \pm 0.50(\text{deg.})$,
$\beta = 1.00(\text{deg.})$, $n = 6.00(rpm)$, $\rho = 2580(kg/m^3)$

7. EFFECT OF FEEDING RATE

Increased feeding rate at fixed values of rotation speed and axis inclination causes increased steady-state bed depth of materials throughout the drum.

Figure 7 shows the variation of bed depth of materials with time at 60 cm distance from feeding section for various amounts of feeding rate, starting from empty drum condition up to achievement of steady state condition. The axis inclination was selected at 1.00(deg.), and the rotation speed at 6.00 rpm. The data show that with increase of feeding rate the bed depth of material decreases.

Figure 8 presents the results of experiments as well as the simulations of the K-C model for the effect of feed flow rate on steady state material bed depth profile. From Figure 8, better fitness of the model and data is seen for higher feeding rates.

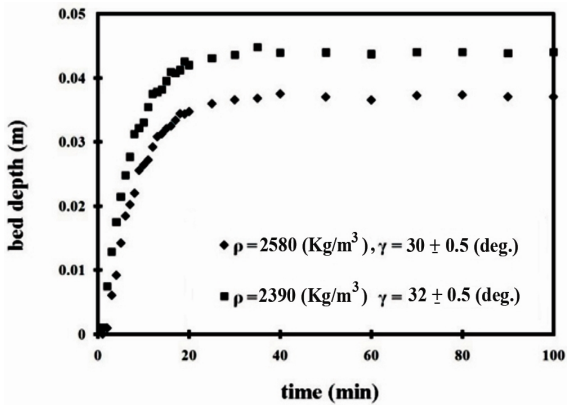

Figure 9. Variation of spent time with powder density for material bed depth to reach to steady state, at 60 cm distance from feeding zone.
$Q_s = 10.33(g/s)$, $\beta = 1.00(\text{deg.})$,
$n = 6.00(rpm)$, $sensor\ \ location = 0.60(m)$

8. EFFECT OF MATERIAL DENSITY

Figures 9 and 10 are drawn to show the effect of density of material (as well as the effect of dynamic angle of repose) on transient bed depth variations and comparisons of steady state bed depth data with that of the K-C model predictions. It is seen from Figure 9 that with increase of density the spent time for filling up of the drum increases. Morever, the steady state of material bed depth also (material filled up) decreases. In the same way, the concluding remark from Figure 10 is that with increase of density, the bed depth profile will decrease, while the predictions of the K-C model are less than that of data.

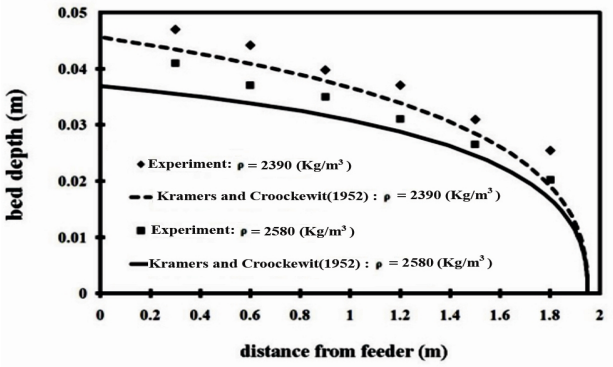

Figure 10. Comparison of predicted values of bed depth by the model of K-C with experimental data(variation of powder density).
$Q_s = 10.33(g/s)$, $\beta = 1.00$ (deg.) , $n = 6.00(rpm)$

9. MATERIAL APEX MOVEMENT

Material apex movement in an empty rotary drum affects the transient filling up of the drums. It is important from the view point of studying transient start-up conditions in rotary drums. In the second part of the paper, this problem will be considered from an empirical modeling view points. From the time of reaching the material apex to any specific cross section the filling up of the drum at that cross section starts and continues up to the time of reaching to a steady state material bed depth. In the following, the effects of feeding rate, rotation speed, axis inclination as well as the material density on the time of material apex movement in an empty drum are investigated and the results are shown in Figures 11 to 14. As are shown in these figures, with increasing of feeding rate, rotation speed and axis inclination, also, with decreasing of material density the speed of movement of the apex of materials in an empty drum increases.

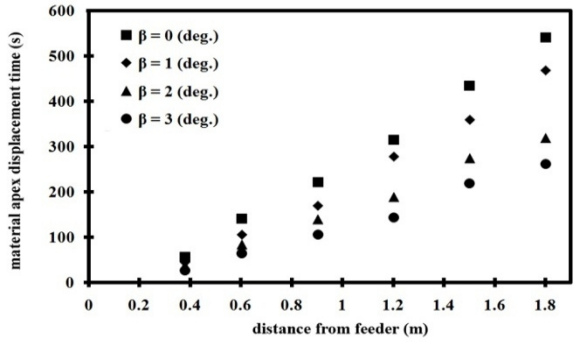

Figure 11. Effect of axis inclination on time of solid materials displacement in the initially empty drum.
$Q_s = 10.33\left(g/s\right)$, $\gamma = 30 \pm 0.50(\text{deg.})$,
$n = 6.00(rpm)$, $\rho = 2580\left(kg/m^3\right)$

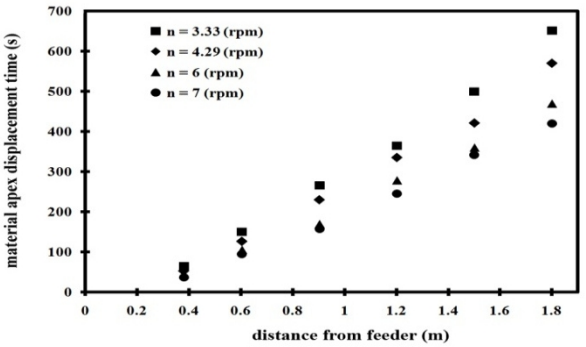

Figure 12. Effect of rotation speed on time of solid materials displacement in the initially empty drum.
$Q_s = 10.33\left(g/s\right)$, $\gamma = 30 \pm 0.50(\text{deg.})$,
$\beta = 1.00^{\circ}(\text{deg.})$, $\rho = 2580\left(g/m^3\right)$

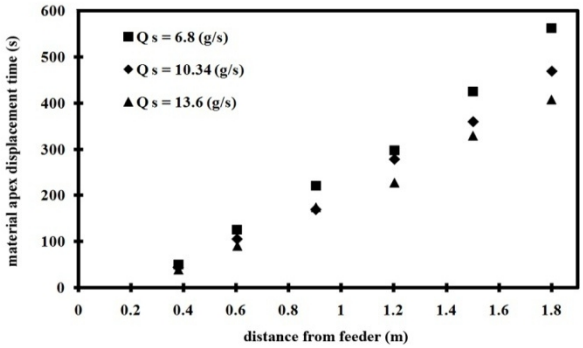

Figure 13. Effect of feed flow rate on time of solid materials displacementin the initially empty drum.
$\gamma = 30 \pm 0.50(\text{deg.})$, $\beta = 1.00(\text{deg.})$,
$n = 6.00(rpm)$, $\rho = 2580\left(g/m^3\right)$

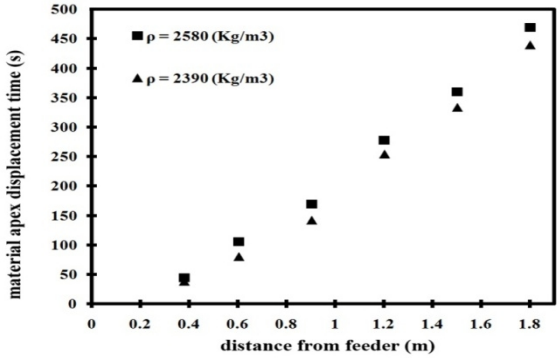

Figure 14. Effect of powder density on time of solid materials displacement in the initially empty drum.
$Q_s = 10.33\left(g/s\right)$, $\gamma = 30 \pm 0.50(\text{deg.})$,
$\beta = 1.00(\text{deg.})$, $n = 6.00(rpm)$

10. MODEL VALIDATION

An overall discussion is presented in this section concerning to the results presented in Figures 4, 6, 8 and 10, which are drawn for the sake of comparing the data with predictions of the K-C model. In Tables 2, 3, 4 and 5 the calculated absolute relative errors with respect to model predictions are summarized. Each of the rows of the tables is related to one set of data as absolute relative errors along the drum that are obtained from experiments and model. The average errors for each row of data are also summarized in the two end columns of each table. In the column before the last one, the average of data for each of the rows of tables are provided for comparison. In the last column averages are presented for the middle four columns excluding the first and the last columns. The last column of data (relevant to 1.80 (m) from feeding section) is excluded in this average since the model of K-C makes use of a nonrealistic boundary condition

which mainly affects the model predictions in the discharge zone. The first column (relevant to 0.30 (m) from feeding section) is also excluded in this set of averages due to particular effects of feeding zone on the bed depth. This effect is mainly resulting from the end wall, existing in the entrance zone of drum, used for prevention of back flow of material. Thus, with the consideration that, more realistic predictions can be obtained from the model in the middle zone of the drum, in addition to the total averages, the averages are provided for the middle four columns, which are reported in the last column. Morever, an average is shown in each table in the lowest row. A comparison of the average values reported in the last two columns of the tables show that, without any exception, in all of the situations the 4 column average values that are related to mid sections are lower than that of 6 column average values, related to overall length of the drum.

TABLE 2. Errors between data and model for variation of axis inclination.

Axis inclination (deg.)	Distance from feeder (m)						Longitudinal average	
	0.3	0.6	1.9	1.2	1.5	1.8	Average of 6 columns	Average of 4 mid columns
0.00	2.42	3.74	3.11	4.10	9.70	41.80	10.83	5.17
1.00	22.81	15.87	15.20	14.22	13.12	30.30	18.59	14.61
2.00	40.61	16.88	28.63	10.76	14.48	14.86	21.04	17.69
3.00	36.52	17.46	25.30	10.90	3.12	4.41	16.29	14.20
Cross Sectional Average	25.59	18.22	13.33	10.65	9.45	22.84		

TABLE 3. Errors between data and model for variation of rotation speed.

Rotation speed (rpm)	Distance from feeder (m)						Longitudinal average	
	0.3	0.6	1.9	1.2	1.5	1.8	Average of 6 columns	Average of 4 mid columns
3.33	4.98	2.85	7.17	5.26	3.27	23.22	7. 80	4.64
4.29	3.98	3.31	1.79	0.28	2.81	20.20	5.40	2.05
6.00	22.81	15.20	15.87	13.12	14.22	30.30	18.59	14.61
7.00	22.22	18.03	10.34	9.30	9.90	23.41	15.54	11.90
Cross Sectional Average	13.50	9.85	8.79	6.99	7.55	24.28		

TABLE 4. Errors between data and model for variation of feed flow rate.

Feed flow rate (g/s)	Distance from feeder (m)						Longitudinal average	
	0.3	0.6	1.9	1.2	1.5	1.8	Average of 6 columns	Average of 4 mid columns
6.80	25.09	31.81	14.03	21.90	14.79	25.00	22.11	18.96
10.33	15.20	22.81	13.12	15.87	14.22	30.30	18.59	14.61
13.60	14.28	6.98	7.33	4.43	5.61	39.44	13.01	6.09
Cross Sectional Average	22.39	15.87	14.92	10.53	11.54	31.58		

TABLE 5. Errors between data and model for variation of powder density.

Powder density (kg / m^3)	Distance from feeder (m)						Longitudinal average	
	0.3	0.6	1.9	1.2	1.5	1.8	Average of 6 columns	Average of 4 mid columns
2580	22.81	15.20	15.87	13.12	14.22	30.30	18.59	14.61
2390	13.25	11.51	10.66	14.66	13.24	48.64	18.66	12.52
Cross Sectional Average	16.76	12.77	13.27	12.47	12.65	36.45		

According to the resulting errors presented in the Table 2, it can be concluded that in low axis inclinations model error is lower for feeding zone compared to that of discharge zone. Contrary to this, with increase of inclination, the condition is vice versa i.e., the error is lower for discharge zone than that of feeding zone. In addition, the errors in the mid sections are almost reasonable comparing to the feeding zone and discharge zone.

From the Table 3, it is seen that the errors relevant to feeding zone are low for low rotation speeds. However, in discharge zone the errors are almost high. The fitness is low at discharge zone. The overall fitness in the mid sections is also moderate. Nevertheless, the overall errors in mid sections are increasing with increase of rotation speed.

Table 4 shows that at lower feeding rates, model fitness is better for discharge zone. While, in higher feeding rates better fitness can be seen for feeding zone and middle zone. However, the fitness is almost weak at discharge zone. The overall conclusion for the mid sections is that with increase of feeding rate the model fitness improves.

The overall conclusion resulting from the data in Table 5 is that with increase of the density the error of feeding section increases, while it decreases in discharge zone. Here, the decrease of error in the discharge zone can be justified in view of the fact that with increase of particle size the bed depth in discharge zone decreases, which makes more compatible situation with the boundary condition used in the model of K-C.

11. CONCLUSIONS

In this paper, the effects of operating variables on bed depth profile in a pilot scale rotary drum are investigated and compared with the predictions of the available model in the literature. The novelty of the paper is that it presents data for fine particles compared to the published data in the literature. Bed depth experimental data gathered from a transparent rotary drum equipped with optical sensors, in accordance with expectations, showed that the steady state bed depth of the K-C model is not good at discharge section due to its unrealistic boundary condition.

Excluding the data obtained for feeding zone and discharge zone, which are both non-adaptable to the mechanistically derivation conditions of the model, for the middle zone data the overall conclusion that can be presented is that the model fitness to the data 1) increases with decrease of axis inclination, 2) increases with decrease of rotation speed, 3) increases with increase of feeding flow rate and 4) almost not affected by the density of material.

However, there is an exceptional operating condition revealed from data. It was related to the highest value of axis inclination in which the minimum value for error at discharge zone was detected. Actually, it was seen that with increase of axis inclination the error of fitting of model for this zone decrease monotonically. This may be argued in the sense that with increase of axis inclination the overall bed depth profile decreases. Thus, it makes the conditions more approached to the boundary condition which is used by Kramers and Croocke within their model.

12. REFERENCES

1. Mastorakos, E., Massias, A., Tsakiroglou, C., Goussis, D., Burganos, V. and Payatakes, A., "Cfd predictions for cement kilns including flame modelling, heat transfer and clinker chemistry", ***Applied Mathematical Modelling***, Vol. 23, No. 1, (1999), 55-76.
2. Spang III, H., "A dynamic model of a cement kiln", ***Automatica***, Vol. 8, No. 3, (1972), 309-323.
3. Kramers, H. and Croockewit, P., "The passage of granular solids through inclined rotary kilns", ***Chemical Engineering Science***, Vol. 1, No. 6, (1952), 259-256.
4. Perron, J. and Bui, R., "Rotary cylinders: Solid transport prediction by dimensional and rheological analysis", ***The Canadian Journal of Chemical Engineering***, Vol. 68, No. 1, (1990), 61-68.
5. Spurling, R., Davidson, J. and Scott, D., "The transient response of granular flows in an inclined rotating cylinder", ***Chemical Engineering Research and Design***, Vol. 79, No. 1, (2001), 51-61.
6. Specht, E., Shi, Y.-C., Woche, H., Knabbe, J. and Sprinz, U., "Experimental investigation of solid bed depth at the discharge end of rotary kilns", ***Powder Technology***, Vol. 197, No. 1, (2010), 17-24.
7. Hamawand, I. and Yusaf, T., "Particles motion in a cascading rotary drum dryer", ***The Canadian Journal of Chemical Engineering***, Vol., No., (2013.(
8. Lebas, E., Hanrot, F., Ablitzer, D. and Houzelot, J.L., "Experimental study of residence time, particle movement and bed depth profile in rotary kilns", ***The Canadian Journal of Chemical Engineering***, Vol. 73, No. 2, (1995), 173-180.
9. Mujumdar, K.S., Ganesh, K., Kulkarni, S.B. and Ranade, V.V., "Rotary cement kiln simulator (rocks): Integrated modeling of pre-heater, calciner, kiln and clinker cooler", ***Chemical Engineering Science***, Vol. 62, No. 9, (2007), 2590-2607.
10. Henein, H., Brimacombe, J. and Watkinson, A" ,.Experimental study of transverse bed motion in rotary kilns", ***Metallurgical transactions B***, Vol. 14, No. 2, (1983), 191-205.

APPENDIX A

According to Figure 2, Points A' and B' are the first and the last sensors in the series of sensors, respectively and C' is a reference fixed sensor located in a minimum point under the bed of material. Surface of the bed can be shown with two points in cross sectional area of the

drum as A and B. The angles φ_1 and φ_2 can be determined by measuring AC' and BC' arc lengths using optical sensors as follows:

$$\varphi_1 = \frac{AC'}{R} \quad (A.1)$$

$$\varphi_2 = \frac{BC'}{R} \quad (A.2)$$

After this point all of the calculations are followed as:

$$\varphi = \frac{\varphi_1 + \varphi_2}{2} \quad (A.3)$$

and

$$\varphi = \frac{1}{2R}(BC' + AC') \quad (A.4)$$

According to Figure 1, the following relations can be written:

$$\varphi + \alpha = \pi / 2 \quad (A.5)$$

$$\alpha + \gamma + \varphi_1 = \pi / 2 \quad (A.6)$$

According to Equations (A.5) and (A.6), dynamic angle of repose can be calculated as:

$$\gamma = \varphi - \varphi_1 \quad (A.7)$$

Furthermore, bed depth of the drum "h" can be calculated as:

$$y = R \cos \varphi \quad (A.8)$$

$$h = R - y \quad (A.9)$$

$$h = R(1 - \cos \varphi) \quad (A.10)$$

Filling degree of materials in a specified cross section can be defined as the ratio of the covered surface by the solid materials to cross sectional area of the drum.

$$S_{solid\ area} = \pi R^2 (\frac{\phi}{\pi}) - \frac{y \times (AB)}{2} \quad (A.11)$$

$$S_{drum} = \pi R^2 \quad (A.12)$$

$$AB = 2R \sin \varphi \quad (A.13)$$

According to Figure 1, calculations of filling degree "j" can be done as following:

$$j = \frac{S_{solid\ area}}{S_{drum}} \times 100 = \frac{\pi R^2 \left(\frac{\phi}{\pi}\right) - \frac{y \times AB}{2}}{\pi R^2} \times 100 \quad (A.14)$$

$$j = \left(\frac{\phi}{\pi} - \frac{R \cos\phi\, R \sin\phi}{\pi R^2}\right) \times 100 = \frac{1}{\pi}\left(\phi - \frac{\sin 2\phi}{2}\right) \times 100 \quad (A.15)$$

Material Flow in Rotary Drums

M. R. Yousefi, M. Shirvani

Department of Chemical Engineering, Iran University of Science & Technology, ResaltCircle, Tehran, Iran

P A P E R I N F O

Paper history:
Received 04 September 2013
Received in revised form 10 November 2013
Accepted 12 December 2013

Keywords:
Rotary Drum;
Material Flow
Steady-State Model
Model Error

چکیده

بررسی آزمایشی جریان مواد در استوانه های دوار فاقد بالا برنده مواد در اشل پایلوت مطالعه شده است. بر خلاف دیگر تحقیقات دیگر انجام شده در مراجع که از مواد دانه درشت استفاده کرده اند ویژگی این مقاله در این است که ذرات ریز دانه در آزمایشات بکار رفته است. هدف اصلی این بوده است که خطاهای مدل یکنواختی که برای بیان حرکت مواد در این دستگاهها مطرح بوده است مشخص گردد. شرایط عملیاتی در آزمایشات برای رژیمهای جریانی slumping، rolling و cascading مورد نظر بوده است. برای برقراری این شرایط دامنه مقادیر سرعت دوران، شیب استوانه و دبی جرمی مواد بترتیب برابر 3.33 to 7.00 (rpm)، 0.00 to 3.00 (deg.) و 6.80 to 13.60 (g/s) مورد استفاده قرار گرفته است. نتایج بدست آمده از بررسی ها نشان میدهند که مدل مطرح شده دارای تطابق ضعیفی برای بیان عمق بستر مواد در ناحیه خوراک و در ناحیه تخلیه می باشد. اما، برای نواحی میانی استوانه نتایج آن قابل قبول است.

doi: *10.5829/idosi.ije.2014.27.06c.02*